Direct detection of antibody–antigen binding using an on-chip artificial pore

Omar A. Saleh and Lydia L. Sohn*

Department of Physics, Princeton University, Princeton, NJ 08544

Communicated by Lewis T. Williams, Five Prime Therapeutics, Emeryville, CA, December 11, 2002 (received for review October 22, 2002)

We demonstrate a rapid and highly sensitive all-electronic technique based on the resistive pulse method of particle sizing with a pore to detect the binding of unlabeled antibodies to the surface of latex colloids. Here, we use an on-chip pore to sense colloids derivatized with streptavidin and measure accurately their diameter increase on specific binding to several different types of antibodies. We show the sensitivity of this technique to the concentration of free antibody and that it can be used to perform immunoassays in both inhibition and sandwich configurations. Overall, our technique does not require labeling of the reactants and is performed rapidly by using very little solution, and the pore itself is fabricated quickly and inexpensively by using soft lithography. Finally, because this method relies only on the volume of bound ligand, it can be generally applied to detecting a wide range of ligand–receptor binding reactions.

Antibodies can be powerful and flexible tools because of their natural ability to bind to virtually any molecule and because of the modern ability to produce specific types in large quantities. These traits have led to the development of a number of important immunosensing techniques in which antibodies of a desired specificity are used to test for the presence of a given antigen (1–4). For example, RIAs have been used in clinical settings to screen for such viruses as hepatitis (5). An integral part of all immunosensing technologies is the ability to detect the binding of antibody to antigen. To accomplish this, most common immunoassays require the labeling of the antibody by using fluorescence, radioactivity, or enzyme activity. However, the need to bind chemically a label to the antibody adds to the time and cost of developing and using these technologies.

Here we report an all-electronic technique for detecting the binding of unlabeled antibody–antigen pairs. Our method is based on the resistive pulse technique of particle sizing (6): a particle passing through a pore displaces conducting fluid, which causes a transient increase, or pulse, in the pore's electrical resistance that in turn is measured as a decrease in current. This technique has been used in the past to measure the size and concentration of a variety of particles, such as cells (7), viruses (8), and colloids (9, 10). More recently, it has been used to detect single molecules (11–13) and their interactions (14). Because the magnitude of the pulse is directly related to the diameter of the particle that produced it (9, 15), we can use the resistive pulse technique to detect the increase in diameter of a latex colloid upon binding to an unlabeled specific antibody. We use this technique to perform two important types of immunoassays: an inhibition assay, in which we detect the presence of an antigen by its ability to disrupt the binding of antibody to the colloid; and a sandwich assay, in which we successively detect the binding of each antibody in a two-site configuration.

Previous particle counting-based immunoassays have used optical or electronic methods to detect the aggregates formed when the antibody crosslinks antigen-coated colloids (16–19). However, relying on crosslinking as a general binding probe is limiting because it requires a free ligand with at least two binding sites. In contrast, our method is more general, because it relies only on the added volume of bound ligand and does not place any limitations on the ligand's functionality. Although it cannot as of yet perform the kinetic analyses that surface plasmon resonance (SPR) techniques (20) are capable of, our device already represents an alternative to SPR for end-point analysis of biological reactions in that it is more rapid, inexpensive, and compact.

We perform our measurements on a chip-based microfluidic device that confers three additional advantages on our system. First, because we have miniaturized the reservoirs leading to the pore, each measurement uses submicroliter quantities of sample and can be performed within minutes. Second, we use common microfabrication and micromolding techniques (21) to make the pore, reservoirs, and electrodes. This allows for quick and inexpensive device construction. Third, using chip-based fabrication can extend the device's capabilities by permitting either future integration of our measurement with other microfluidic components (22, 23) such as separation units or mixers, or construction of arrays of sensors on a single chip for performing many measurements or assays in parallel.

Methods

Fig. 1 shows a picture of our device: a polydimethylsiloxane (PDMS) mold sealed to a glass coverslip. The PDMS mold is cast from a master (21) and contains two reservoirs (7 μm deep, 400 μm wide) connected to an embedded pore (typically 7–9 μm long and 1 μm in diameter). The glass coverslip has platinum electrodes that extend across the width of the reservoirs and are fabricated on the glass coverslip before PDMS sealing. These electrodes are used to perform the electronic measurement. We prepare both the PDMS slab and the coverslip by using standard lithographic, micromolding, and metal deposition techniques (see *Supporting Text*, which is published as supporting information on the PNAS web site, www.pnas.org). Solution is added to the reservoirs via two holes cut through the PDMS slab, and capillary action is used to initially draw the solution through both reservoirs and the pore. Pressure is applied to the access holes after loading the solution to drive the suspended latex colloids through the pore.

All solutions are mixed in 0.5× PBS, pH 7.3, and contain 0.05% Pluronics F127 surfactant (a nonionic surfactant) and 0.2 mg/ml BSA. The BSA and surfactant are added to decrease both sticking of colloids to the device walls and nonspecific adhesion of antibodies to the particles. We prepare a stock colloidal solution by mixing and twice centrifugally rinsing the colloids in the above buffer. This stock solution is then diluted by a factor of 10 and mixed with the relevant antibodies and/or antigens before each measurement. For the sandwich assay, we attach biotinylated antibody to streptavidin colloids by incubating a high concentration of the biotinylated antibody with the stock solution, then centrifugally rinsing to remove unbound molecules. Some solutions are passed through a 0.8-μm pore size filter immediately before measuring so as to remove aggregates caused by the crosslinking of the colloids by the antibody.

Once each device is loaded with the solution to be analyzed, we measure the current through the pore at constant applied DC

Abbreviation: PDMS, polydimethylsiloxane.

*To whom correspondence should be addressed. E-mail: sohn@princeton.edu.

 www.pnas.org/cgi/doi/10.1073/pnas.0337563100

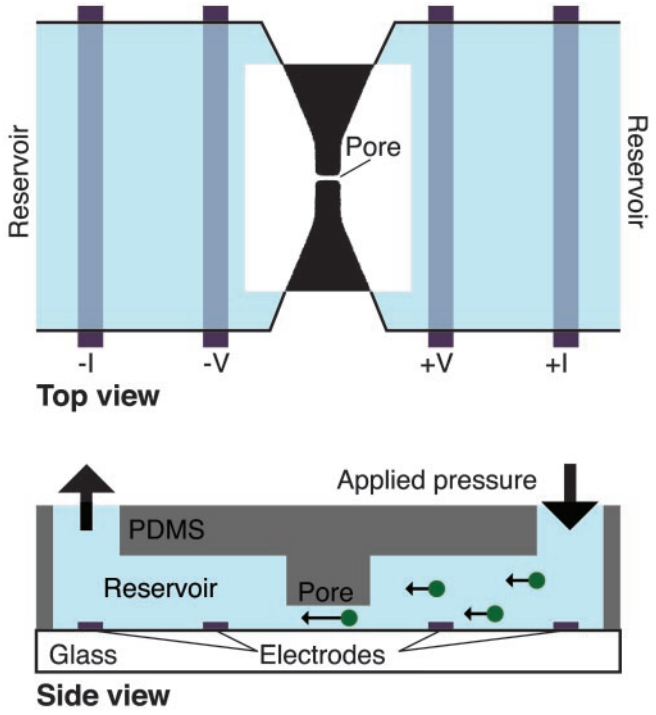

Fig. 1. Schematic side and top views of our device. We create the device by sealing a PDMS mold (containing two reservoirs connected by a pore) to a glass coverslip, and then filling it with solution. Pressure is used to drive the particles through the pore. The electrical current across the pore is measured at constant applied voltage by using a four-point technique, where the inner (outer) electrodes control the voltage (current). Incorporated into the top view is an optical image of an actual sealed device containing a 7-μm-long, 1-μm-wide pore.

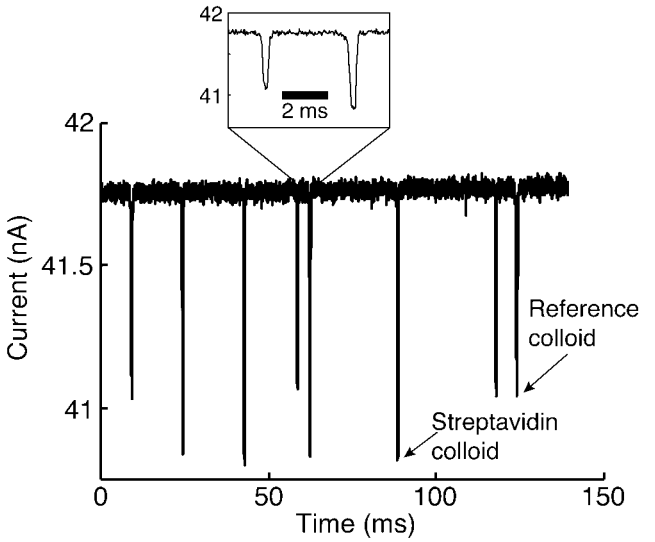

Fig. 2. A typical measurement of the current across a pore as different colloids pass through it. Each downward pulse corresponds to a single colloid transiting the pore. There is a clear difference in pulse magnitude as a result of the difference in size of the streptavidin colloids as compared with the reference colloids. This difference allows us to separate the pulses for pore calibration (see text). (*Inset*) An expanded view of two pulses. As shown, they are well resolved in time and consequently allow an unambiguous measurement of the pulse height. The data shown were taken with an applied voltage of 0.4 V and a pressure of ≈6.9 kPa.

voltage (0.2–0.5 V). Fig. 2 shows a typical measurement of the current: each downward pulse corresponds to a single colloid passing through the pore. Particle transit times are typically ≈200 μs when a pressure of ≈7 kPa (≈1 psi) is applied. Such transit times are long enough to establish a stable square pulse shape (see Fig. 2 *Inset*). We measure several hundred colloids in a given solution during a single experimental run, after which the device is either cleaned appropriately and reused or discarded. Custom-written software is used to extract both the height and width of each pulse in a trace. As described (24), the accuracy of the measurement is increased by using the measured width of each pulse to correct for the effect on the pulse height of a particle traveling off of the pore axis (25, 26).

Discussion

The goal of this work is to detect an increase in the magnitude of the pulses caused by the volume increase when ≈510-nm diameter streptavidin-coated latex colloids specifically bind to antibodies. The relative height of a pulse $\delta I/I$, where δI is the absolute pulse height and I is the baseline current value, depends on the relation of the diameter d of each colloid to the diameter D and length L of the pore (9, 15, 27–29). For the values of d (≈510 nm) and D (≈900 nm) used here, this relation is described by:

$$\left|\frac{\delta I}{I}\right| = \frac{D}{L}\left[\frac{\arcsin(d/D)}{\sqrt{1-(d/D)^2}} - \frac{d}{D}\right]. \qquad [1]$$

Using this equation, we can determine d for each streptavidin colloid measured if we know the dimensions of the pore. We directly measure L with an optical microscope. However, we cannot directly measure the pore's diameter D; instead, we perform a calibration by adding a reference colloid of known diameter (a 470-nm diameter sulfate-coated latex colloid) to each solution of streptavidin colloids. The absolute difference in diameter (470–510 nm) between the two types of colloids results in a clear difference in the pulse heights (see Fig. 2); consequently, we can determine easily which size colloid produced each pulse. We use the values of $\delta I/I$ arising from the reference colloids, along with the known values of L and d, to invert numerically Eq. **1** to thus determine the pore diameter D. Once this is accomplished, we use Eq. **1** once again to correlate the magnitude of each pulse to the diameter of the streptavidin colloid that produced it.

Fig. 3*a* shows a histogram comparing the distribution of measured colloid diameters obtained from two different solutions: one containing only the streptavidin and the reference colloids, and one containing both types of colloids and 0.1 mg/ml monoclonal mouse antistreptavidin antibody (with an affinity for streptavidin $>10^{10}$). As shown, there is a clear increase of 9 nm in the diameter of the streptavidin colloids in the solution containing the antibody (see also Fig. 3*b*). We attribute this increase to the volume added to the colloid on the specific binding to the antistreptavidin. Specificity is demonstrated by the much smaller increase in diameter (≈2.5 nm) when mixing the colloids with 0.1 mg/ml monoclonal isotype-matched irrelevant antibody (mouse anti-rabbit; see Fig. 3*b*). This smaller increase is a result of nonspecific binding of the irrelevant antibody to the colloids.

In Fig. 4 we show the measured change in colloid diameter as the concentration of the specific, high-affinity antibody (monoclonal antistreptavidin) is varied from 0.1 μg/ml to 100 μg/ml. As shown, the colloid diameter reaches its maximum value when the colloids are mixed with ≥5 μg/ml antibody. Using a Bradford protein assay (30), we determined the minimum saturating concentration of antibody for the colloid concentration in our experiment (1.2×10^9 particles per ml) to be 3.5 μg/ml, which is in good agreement with the results of our electronic pore-

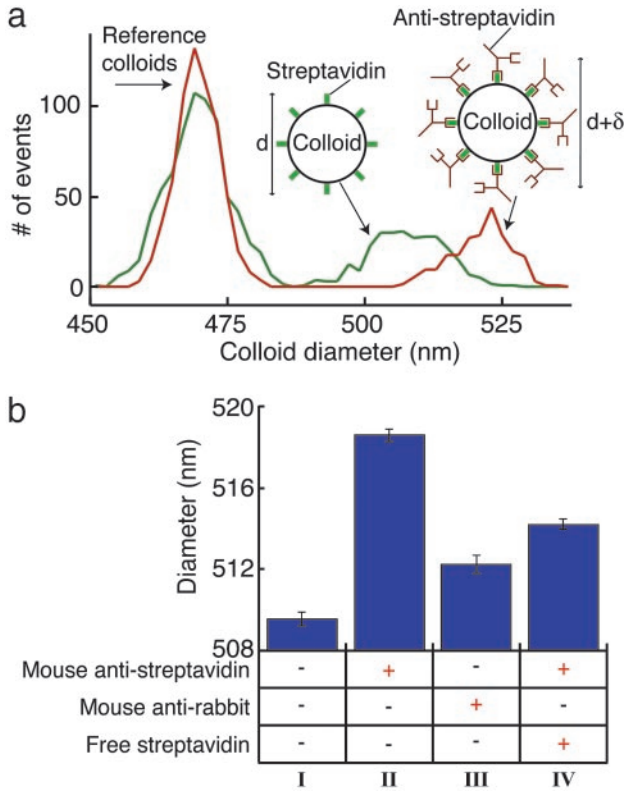

Fig. 3. (*a*) A histogram showing the distribution of colloid diameters measured from a solution that contains only the reference and streptavidin colloids (green line) and a solution that contains both types of colloids and 0.1 mg/ml monoclonal antistreptavidin antibody (red line). The specific binding of antistreptavidin to the streptavidin colloids produces a clear increase in the diameter of the colloids. (*b*) A summary of the measurements of the mean diameter of the streptavidin colloids when mixed in different solutions. A single experimental run consists of measuring several hundred colloids of each type in one solution; the plotted bars represent the mean diameter extracted from three to five such runs on the same solution, but using different devices. All solutions contained the streptavidin colloids and the reference colloids in a 0.5× PBS buffer (pH 7.3). The presence of additional components in each solution is indicated by a + in the column beneath the plotted bar. Column I shows the mean diameter measured without any protein added to the solution. A 9-nm increase in colloid diameter is seen in the presence of the specific antibody to streptavidin (0.1 mg/ml mouse antistreptavidin, column II); we attribute this to the volume added to the colloid caused by the specific binding of the antibody. The specificity of the probe is shown by the lack of a similar diameter increase in the presence of isotype-matched irrelevant antibody (0.1 mg/ml mouse anti-rabbit, column III); the small diameter increase in this solution can be attributed to nonspecific adhesion. We also perform an inhibition assay, where the specific binding of the antistreptavidin to the colloid is disrupted by the presence of 0.2 mg/ml free streptavidin (column IV) (the presence of free antigen is shown by the decrease in diameter compared with the antigen-free solution, column II). The error bars in all figures represent the uncertainty in determining the mean diameter based on one standard deviation of the measured distributions. The dominant source of error in our measurements is the intrinsic distribution in the streptavidin colloids' diameter, with smaller contributions from the spread in diameter of the reference colloids and the electrical noise in the current measurement.

based immunoassay. Furthermore, the manufacturer-quoted binding capacity of the colloids indicates that each colloid has ≈9,800 streptavidin molecules on its surface. If each colloid binds to an equivalent number of antibodies, the minimum saturating concentration for a solution containing 1.2×10^9 colloids/ml will be ≈3.0 μg/ml; again, this finding is in good agreement with our results. As shown in Fig. 4, the dynamic range of our assay corresponds to antibody concentrations from

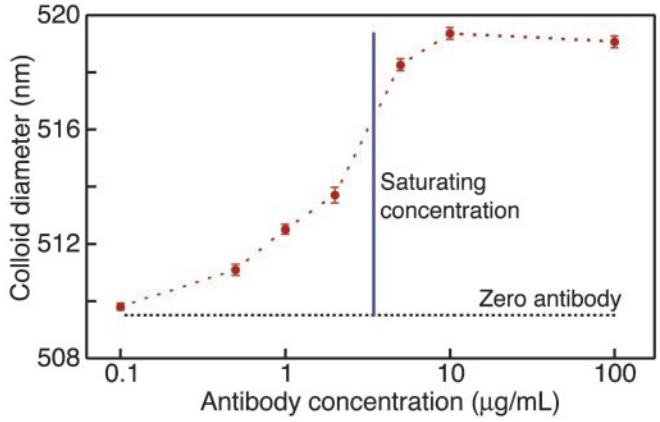

Fig. 4. Measurements of the mean colloid diameter when mixed in solutions of varying monoclonal mouse antistreptavidin concentrations. The vertical line marks the binding capacity of the colloids as determined by a Bradford protein assay. The diameter of the colloids in the absence of antibody is shown as the black dashed line.

0.5 μg/ml to the saturating concentration of ≈5 μg/ml. By decreasing the colloid concentration, we can decrease the binding capacity of the solution, thus decreasing the saturating concentration of antibody. In this manner, we can expect the range of sensitivity of the device to decrease to antibody concentrations as low as 10–50 ng/ml.

We use our technique's ability to detect successfully the specific binding of unlabeled antibodies to the colloids to perform an inhibition immunoassay. We measure a 4.5-nm increase (see column IV of Fig. 3*b*) in the diameter of the streptavidin colloids when mixed with 0.1 mg/ml antistreptavidin that had been preincubated with 0.2 mg/ml free streptavidin. This smaller increase (relative to the solution containing only antistreptavidin) indicates a decrease in the number of antibodies binding to each colloid. We primarily attribute this to the free streptavidin blocking the antibody binding sites. The measured diameter of the streptavidin-coated colloid therefore indicates the presence of free streptavidin in the solution. In general, this inhibition method can be extended to detect any antigen that can be immobilized on the colloid surface.

The 4.5-nm increase seen in column IV of Fig. 3*b* shows that some binding of antibody to the colloid does in fact occur. Based on the control measurement with an irrelevant antibody (column III of Fig. 3*b*), we attribute this increase to a combination of nonspecific binding of blocked antibodies and incomplete inhibition of the antibody by the free streptavidin. The possibility of nonspecific binding does decrease the dynamic range of the measurement. However, because of the very small uncertainty in the measured mean colloid diameter, the dynamic range necessary to determine the amount of ligand bound to the colloid is still quite large.

As a second demonstration of our technique's high sensitivity to the volume added by molecules bound to a streptavidin colloid, we perform an immunoassay (summarized in Fig. 5) with a sandwich configuration. Here, a primary antibody that is immobilized on the colloid surface binds to a free antigen, which in turn is bound to a secondary antibody. We immobilize the primary antibody by mixing streptavidin colloids with a biotinylated antibody (rabbit anti-*Streptococcus* group A) to thus create a colloid–antibody conjugate through the streptavidin–biotin bond. As shown in Fig. 5, the measured conjugated colloids are 514 nm in diameter, a 5-nm increase over the "bare" streptavidin colloids. Next, we mix the colloid–antibody conjugates with both the specific antigen to the primary antibody (extract from a culture of *Streptococcus* group A) and 0.1 mg/ml

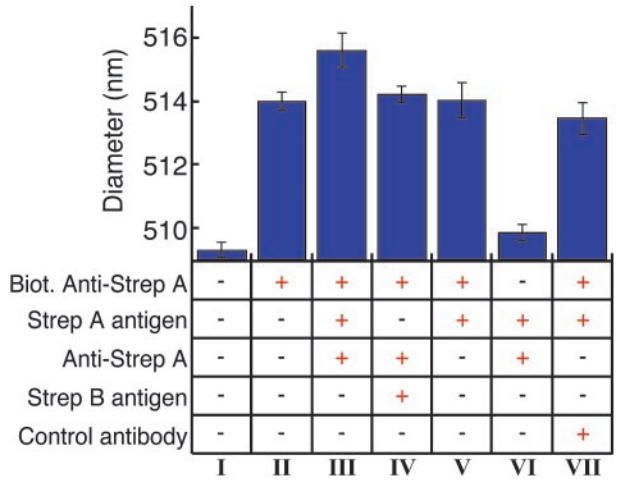

Fig. 5. Summary of the mean colloid diameters measured when forming an antibody–antigen–antibody ''sandwich'' on the colloid surface. All solutions contain the reference and streptavidin colloids in a 0.5× PBS buffer (pH 7.3), along with additional components as indicated by the + in the column below the plotted bar. Column I indicates the measured diameter of the bare streptavidin colloid. We measure a ≈5-nm increase (column II) in diameter after conjugating a biotinylated antibody (biotinylated anti-*Streptococcus* group A) to the streptavidin-coated colloids. A further increase of ≈1.6 nm is seen (column III) when adding both extract from a culture of *Streptococcus* group A and a secondary antibody specific to that antigen (unlabeled anti-*Streptococcus* group A); this increase indicates the formation of the sandwich on the colloid surface. The specificity of the configuration is shown by the lack of an increase in diameter when adding extract from a culture of *Streptococcus* group B (which is not bound by either antibody) in place of the group A extract (column IV), or an irrelevant antibody in place of the specific secondary antibody (column VII). When adding the specific antigen and secondary antibody to unconjugated colloids (column VI), we measure no significant diameter increase, indicating that nonspecific adhesion of antigen–secondary antibody complexes are not the cause of the diameter increase seen in column III. Finally, when adding the specific antigen alone to the conjugated colloids (column V), we see no increase in diameter, indicating that the diameter increase in column III is primarily caused by the binding of the secondary antibody.

secondary antibody (unlabeled rabbit anti-*Streptococcus* group A). Measurements of this solution show the colloids further increase in diameter by 1.6 nm. This 1.6-nm increase is not seen when the colloids are mixed with the antigen alone, indicating that the binding of the secondary antibody is the principal reason for the diameter increase. The specificity of this arrangement is demonstrated by the absence of a diameter increase in the control measurements we perform in which either the antigen or the secondary antibody is replaced by nonspecific counterparts (see Fig. 5).

It is intriguing that the measured 5-nm increase after attachment of the biotinylated antibody is less than the maximum 9-nm increase seen when using the antibody–antigen bond (Figs. 3 and 4) to attach antibody to the colloid. This surprising difference is most likely caused by the differing conformations of the antibody in each case; however, further work is needed to clarify this. Nonetheless, despite the smaller size increase, the ability of the device to perform the sandwich assay is still clearly demonstrated.

Although we have used an antibody/antigen reaction to demonstrate the power of our technique, we emphasize that its true strength is its generality: it does not rely on any functional properties of the free ligand. Thus, it can be applied to any ligand/receptor pair, provided the free ligand is large enough to produce a discernible change in the size of the colloid.

Future work on the device should focus on optimizing its sensitivity in terms of both ligand size (mass) and concentration. The sensitivity depends on four factors: the amount of ligand bound to each colloid, the intrinsic dispersion in colloid size, the colloid geometry, and the colloid concentration. First, increasing the number of binding sites will lead to more ligands bound per colloid, and consequently a larger change in size. For the colloids used here, the parking area for each binding site is ≈80 nm^2; although this is close to the steric limit for antibody molecules, the use of a smaller ligand would permit more binding sites per colloid. Second, the intrinsic spread in the sizes of the streptavidin colloids is the largest source of error in our measurement. The device's sensitivity would be enhanced by using a more monodisperse population of colloids (one with a coefficient of variation in diameter of <2%), or even a solution of highly monodisperse nanocrystals (31). Third, at constant binding density, the measured change in pulse height on binding to free ligand is proportional to the surface-to-volume ratio of the colloid. Thus, we could increase the sensitivity and dynamic range of the assay by using a smaller colloid. For example, we estimate that using a colloid 250 nm in diameter would increase the sensitivity of the assay by a factor of 4 in either ligand size or concentration. Thus, based on the data shown in Fig. 4, using a 250-nm colloid at the same particle concentration used in this article would make the assay sensitive to either 38-kDa ligand molecules at concentrations of 0.5 μg/ml or antibody concentrations near 0.1 μg/ml. We mention that an even more effective strategy to increase the surface-to-volume ratio would be to use a nonspherical or porous colloid (assuming the pore size is large enough to admit the free ligand) as the substrate for the immobilized receptor. Fourth, as previously mentioned, decreasing the concentration of colloids would further increase the sensitivity because it would decrease the minimum saturating concentration of free ligand. Overall, a combination of these four strategies should result in the increased sensitivity of our assay to ligand concentrations at or below 1 ng/ml.

In conclusion, we have demonstrated our ability to use an electronic measurement to detect the binding of unlabeled antibodies to the surface of latex colloids. This ability is generally applicable to determining rapidly and precisely the thickness of a layer of any kind of biological macromolecule bound to a colloid. Here, we specifically showed that our technique can be used to perform two widely used and important immunoassays (an inhibition assay and sandwich assay) in which either the antigen or antibody is immobilized on the colloid. In contrast to how these assays are performed today, ours requires no labeling of analytes, uses only submicroliter volumes of sample, and can be performed rapidly and inexpensively. For instance, we have compared our technique's ability (using a sandwich configuration) to detect the presence of *Streptoccocus* group A to that of a standard latex agglutination assay. We have found our method to be an order of magnitude more sensitive and more than four times as fast as the agglutination assay. Overall, our device can be used to detect many different kinds of analytes, because the colloids can be easily modified to have almost any specificity (through, for example, the biotin–streptavidin interaction used here). Furthermore, our technique can be extended to multianalyte detection not only by using several microparticles with different chemical sensitivities and different mean diameter but also by using devices consisting of arrays of pores (O.A.S., L. Dunkelberger, and L.L.S., unpublished work). Finally, in addition to a host of biosensing applications, this technique can be used as a diagnostic test of the surface chemistry of colloids.

We thank L. T. Williams, D. Notterman, D. Charych, and R. Halenbeck for helpful discussions. This work was supported in part by the National Science Foundation, Defense Advanced Research Projects Agency, and Army Research Office. O.A.S. acknowledges support from the Fannie and John Hertz Foundation.

1. Luppa, P. B., Sokoll, L. J. & Chan, D. W. (2001) *Clin. Chim. Acta* **314,** 1–26.
2. Vo-Dinh, T. & Cullum, B. (2000) *Fresenius J. Anal. Chem.* **366,** 540–551.
3. Turner, A. P. (2000) *Science* **290,** 1315–1317.
4. Stefan, R. I., van Staden, J. F. & Aboul-Enein, H. Y. (2000) *Fresenius J. Anal. Chem.* **366,** 659–668.
5. Ngo, T. T. (2000) *Methods* **22,** 1–3.
6. Coulter, W. H. (1953) U.S. Patent No. 2,656,508.
7. Kubitschek, H. E. (1958) *Nature* **182,** 234–235.
8. Deblois, R. W. & Wesley, R. K. A. (1977) *J. Virol.* **23,** 227–233.
9. Deblois, R. W. & Bean, C. P. (1970) *Rev. Sci. Instrum.* **41,** 909–913.
10. Deblois, R. W., Bean, C. P. & Wesley, R. K. A. (1977) *J. Colloid Interface Sci.* **61,** 323–335.
11. Li, J., Stein, D., McMullan, C., Branton, D., Aziz, M. J. & Golovchenko, J. A. (2001) *Nature* **412,** 166–169.
12. Bayley, H. & Cremer, P. S. (2001) *Nature* **413,** 226–230.
13. Bezrukov, S. M., Vodyanoy, I. & Parsegian, V. A. (1994) *Nature* **370,** 279–281.
14. Gu, L. Q., Cheley, S. & Bayley, H. (2001) *Science* **291,** 636–640.
15. Saleh, O. A. & Sohn, L. L. (2001) *Rev. Sci. Instrum.* **72,** 4449–4451.
16. Sykulev, Y. K., Sherman, D. A., Cohen, R. J. & Eisen, H. N. (1992) *Proc. Natl. Acad. Sci. USA* **89,** 4703–4707.
17. von Schulthess, G. K., Benedek, G. B. & Deblois, R. W. (1983) *Macromolecules* **16,** 434–440.
18. von Schulthess, G. K., Benedek, G. B. & Deblois, R. W. (1980) *Macromolecules* **13,** 939–945.
19. von Schulthess, G. K., Deblois, R. W. & Benedek, G. B. (1978) *Biophys. J.* **21,** A115–A115.
20. Mullett, W. M., Lai, E. P. & Yeung, J. M. (2000) *Methods* **22,** 77–91.
21. Xia, Y. N. & Whitesides, G. M. (1998) *Angew. Chem. Int. Ed.* **37,** 551–575.
22. Whitesides, G. M. & Stroock, A. D. (2001) *Phys. Today* **54,** 42–48.
23. Chovan, T. & Guttman, A. (2002) *Trends Biotechnol.* **20,** 116–122.
24. Saleh, O. A. & Sohn, L. L. (2002) *Rev. Sci. Instrum.* **73,** 4396–4398.
25. Berge, L. I., Jossang, T. & Feder, J. (1990) *Meas. Sci. Technol.* **1,** 471–474.
26. Smythe, W. R. (1972) *Rev. Sci. Instrum.* **43,** 817–818.
27. Gregg, E. C. & Steidley, K. D. (1965) *Biophys. J.* **5,** 393–405.
28. Anderson, J. L. & Quinn, J. A. (1971) *Rev. Sci. Instrum.* **42,** 1257–1258.
29. Smythe, W. R. (1964) *Phys. Fluids* **7,** 633–638.
30. Bradford, M. M. (1976) *Anal. Biochem.* **72,** 248–254.
31. Bruchez, M., Jr., Moronne, M., Gin, P., Weiss, S. & Alivisatos, A. P. (1998) *Science* **281,** 2013–2016.